AIP Applied Physics Letters

The adsorption-controlled growth of LuFe2O4 by molecular-beam epitaxy

Charles M. Brooks, Rajiv Misra, Julia A. Mundy, Lei A. Zhang, Brian S. Holinsworth, Kenneth R. O'Neal, Tassilo Heeg, Willi Zander, J. Schubert, Janice L. Musfeldt, Zi-Kui Liu, David A. Muller, Peter Schiffer, and Darrell G. Schlom

Citation: Applied Physics Letters **101**, 132907 (2012); doi: 10.1063/1.4755765
View online: http://dx.doi.org/10.1063/1.4755765
View Table of Contents: http://scitation.aip.org/content/aip/journal/apl/101/13?ver=pdfcov
Published by the AIP Publishing

Articles you may be interested in
Direct band gaps in multiferroic h-LuFeO3
Appl. Phys. Lett. **106**, 082902 (2015); 10.1063/1.4908246

Adsorption-controlled growth of BiVO4 by molecular-beam epitaxy
APL Mat. **1**, 042112 (2013); 10.1063/1.4824041

Ferroic investigations in LuFe2O4 multiferroic ceramics
J. Appl. Phys. **110**, 034108 (2011); 10.1063/1.3622147

Adsorption-controlled growth of BiMnO 3 films by molecular-beam epitaxy
Appl. Phys. Lett. **96**, 262905 (2010); 10.1063/1.3457786

Adsorption-controlled molecular-beam epitaxial growth of Bi Fe O 3
Appl. Phys. Lett. **91**, 071922 (2007); 10.1063/1.2767771

Want to publish your paper in the
#1 MOST CITED journal in applied physics?
With Applied Physics Letters, you can.
AIP Applied Physics Letters
THERE'S POWER IN NUMBERS. Reach the world with AIP Publishing.

This article is copyrighted as indicated in the article. Reuse of AIP content is subject to the terms at: http://scitation.aip.org/termsconditions. Downloaded to IP: 128.84.143.26 On: Mon, 27 Apr 2015 14:52:39

The adsorption-controlled growth of $LuFe_2O_4$ by molecular-beam epitaxy

Charles M. Brooks,[1,2] Rajiv Misra,[3] Julia A. Mundy,[4] Lei A. Zhang,[2] Brian S. Holinsworth,[5] Kenneth R. O'Neal,[5] Tassilo Heeg,[1] Willi Zander,[6] J. Schubert,[6] Janice L. Musfeldt,[5] Zi-Kui Liu,[2] David A. Muller,[4,7] Peter Schiffer,[3] and Darrell G. Schlom[1,7]
[1]*Department of Materials Science and Engineering, Cornell University, Ithaca, New York 14853-1501, USA*
[2]*Department of Materials Science and Engineering, Pennsylvania State University, University Park, Pennsylvania 16802, USA*
[3]*Department of Physics and Materials Research Institute, Pennsylvania State University, University Park, Pennsylvania 16802, USA*
[4]*School of Applied and Engineering Physics, Cornell University, Ithaca, New York 14853, USA*
[5]*Department of Chemistry, University of Tennessee, Knoxville, Tennessee 37996, USA*
[6]*Peter Gruenberg Institut (PGI-9), JARA-Fundamentals of Future Information Technologies, Research Centre Jülich, D-52425 Jülich, Germany*
[7]*Kavli Institute at Cornell for Nanoscale Science, Ithaca, New York 14853, USA*

(Received 5 June 2012; accepted 13 September 2012; published online 28 September 2012)

We report the growth of single-phase (0001)-oriented epitaxial films of the purported electronically driven multiferroic, $LuFe_2O_4$, on (111) $MgAl_2O_4$, (111) MgO, and (0001) 6H-SiC substrates. Film stoichiometry was regulated using an adsorption-controlled growth process by depositing $LuFe_2O_4$ in an iron-rich environment at pressures and temperatures where excess iron desorbs from the film surface during growth. Scanning transmission electron microscopy reveals reaction-free film-substrate interfaces. The magnetization increases rapidly below 240 K, consistent with the paramagnetic-to-ferrimagnetic phase transition of bulk $LuFe_2O_4$. In addition to the $\sim$0.35 eV indirect band gap, optical spectroscopy reveals a 3.4 eV direct band gap at the gamma point. *© 2012 American Institute of Physics*. [http://dx.doi.org/10.1063/1.4755765]

The quest for multiferroics, materials where magnetic order and ferroelectricity coexist, has been challenging due to the frequent incompatibility of the two phenomena.[1,2] Reports that $LuFe_2O_4$ is simultaneously ferrimagnetic and ferroelectric below 250 K, the highest temperature of any known material,[3] have resulted in significant interest in $LuFe_2O_4$. Of late, however, the multiferroic status of $LuFe_2O_4$ has become controversial.[4–7] Unlike more traditional ferroelectrics, $LuFe_2O_4$ has been reported to develop a ferroelectric polarization from the charge ordering of Fe^{2+} and Fe^{3+} ions.[3] This charge ordering mechanism would make $LuFe_2O_4$ an improper ferroelectric, free of a requisite polar displacement that often precludes the presence of magnetism.[2] On the other hand, recent experiments have shown that such charge ordering is absent in $LuFe_2O_4$,[4] that it is not ferroelectric,[5] and further that the antiferromagnetic order seen in some single crystals[6] could imply the ferrimagnetic order seen in many samples is due to non-stoichiometry.

The ability to deposit single-crystal thin films of $LuFe_2O_4$ is a key stepping stone on the path to understanding and manipulating the properties of this material, for example, with strain.[8,9] There has been some success with growing thin films of $LuFe_2O_4$ by pulsed-laser deposition (PLD),[10–12] though so far this achievement is limited to polycrystalline films or films with impurity phases present, particularly at the interface. In these cases, the desired $LuFe_2O_4$ phase only forms with excess iron present during growth by PLD.[11] Primary challenges to the growth of higher quality films include the sensitivity of the growth process to substrate temperature and oxygen pressure as well as a lack of suitable substrates.

In this work, we report the deposition of $LuFe_2O_4$ thin films by molecular-beam epitaxy (MBE) using an adsorption controlled growth process to control the film composition. The growth method is inspired by that used in the growth of GaAs by MBE.[13–15] This thermodynamically driven process allows the composition of GaAs to self-limit to the stoichiometric value over a limited growth temperature range despite the substrate being supplied with excess arsenic. A similar process has also been employed as a method of composition-control in MBE-grown oxide thin films of compounds, such as $PbTiO_3$ and $BiFeO_3$.[16,17] In the case of oxides, oxygen background pressure and substrate temperature are the parameters that define the growth window where stoichiometric film deposition occurs. The growth of $LuFe_2O_4$ is analogous to that of $InFe_2O_4$, which has been achieved in a similar manner at lower temperature using PLD by making use of the volatility of indium at the growth conditions.[18] Here, we use the volatility of iron oxides to achieve phase-pure $LuFe_2O_4$ by adsorption-controlled growth.

The first step toward achieving epitaxial deposition of $LuFe_2O_4$ films was uncovering a growth window. The thermodynamic properties of individual phases in the Fe-Lu-O system were developed by means of the CALPHAD method[19] and the phase diagram was calculated using Thermo-Calc[20] with a molar ratio of Fe:Lu of 2. These calculations provided the temperature and pressure region where the formation of $LuFe_2O_4$ is favorable, shown in Fig. 1.

Finding viable substrates providing a suitable template for single-phase epitaxial films of $LuFe_2O_4$ is also critical. Of commercially available substrates, we identified (111) MgO, (111) $MgAl_2O_4$, and (0001) 6H-SiC as candidates for the growth of (0001) $LuFe_2O_4$ films. The observed epitaxial relationship between (0001) $LuFe_2O_4$ and the various substrates is shown in Fig. 2(b). The lattice mismatch values for

 © 2012 American Institute of Physics

This article is copyrighted as indicated in the article. Reuse of AIP content is subject to the terms at: http://scitation.aip.org/termsconditions. Downloaded to IP: 128.84.143.26 On: Mon, 27 Apr 2015 14:52:39

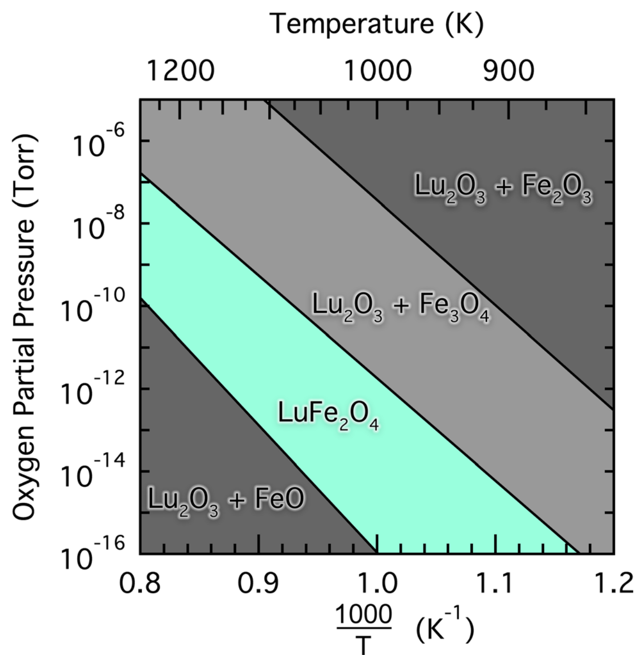

FIG. 1. Arrhenius plot of oxygen partial pressure vs. reciprocal temperature showing where $LuFe_2O_4$ is thermodynamically stable.

$LuFe_2O_4$ films on MgO, $MgAl_2O_4$, and SiC are −15.5%, −4.25%, and −12.0%, respectively.[21,22]

Using the phase diagram in Fig. 1 as a guide to the adsorption-controlled regime, $LuFe_2O_4$ films were grown using a Veeco GEN 10 MBE system dedicated to the growth of oxides at a growth temperature of $850 \pm 20\,°C$ as measured by optical pyrometry in a background pressure of $\sim 1.0 \times 10^{-6}$ Torr of molecular oxygen. Effusion cells were used to provide elemental fluxes of lutetium and iron. Epitaxial films of $LuFe_2O_4$ were successfully grown on (111) MgO, (111) $MgAl_2O_4$, and (0001) 6H-SiC single crystal substrates. Films were typically grown to a thickness of 50 nm and prepared with thicknesses up to 75 nm for optical measurements. In order to ensure the growth of a stoichiometric film, excess iron is required during the deposition process. At a growth temperature of 850 °C, much of the supplied iron is evaporated as Fe_xO_y species and is not incorporated into the resulting film. Source fluxes were determined using a quartz crystal microbalance prior to growth. Film structure was monitored periodically throughout the growth by reflection high-energy electron diffraction (RHEED). The lutetium and iron source fluxes were 6.0×10^{12} atoms/(cm^2 s) and 2.4×10^{13} atoms/(cm^2 s), respectively, corresponding to an overall lutetium-limited growth rate of ∼3.2 Å/min. Although the amount of iron supplied is twice that required for the $LuFe_2O_4$ structure, the excess iron is not incorporated into the film. Rutherford backscattering spectrometry (RBS) was used to verify that the Lu:Fe stoichiometry of the films is indeed 1:2 and that the sticking coefficient of iron is lower at high growth temperatures in the same oxygen background pressure used for the growth of $LuFe_2O_4$ films.

Four-circle x-ray diffraction (XRD) was performed using a high-resolution Philips X'Pert Pro MRD diffractometer with a PreFix hybrid monochromator on the incident side and triple axis/rocking curve attachment on the diffracted side.

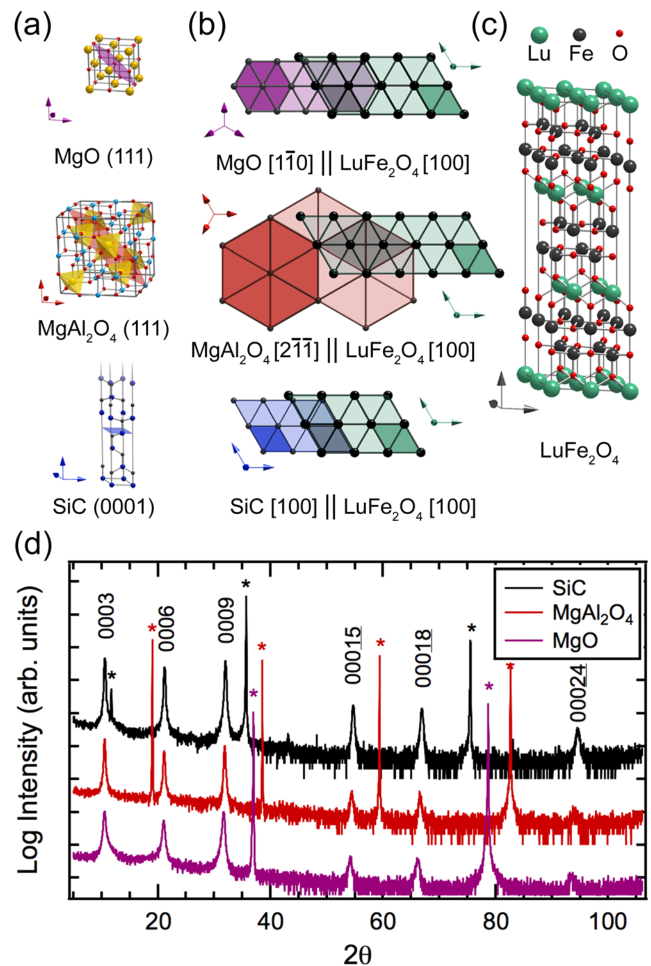

FIG. 2. (a) Substrate model for MgO, $MgAl_2O_4$, and 6H-SiC with the (111), (111), and (0001) planes of the substrate surface highlighted, respectively. (b) The epitaxial orientation relationship of a $LuFe_2O_4$ lattice on (111) MgO, (111) $MgAl_2O_4$, and (0001) 6H-SiC lattices (see Ref. 21). (c) A model showing the alternating single layers of lutetium oxide (U layers, Ref. 24) and double layers of iron oxide (W layers, Ref. 24) in $LuFe_2O_4$. (d) θ-2θ x-ray diffraction scans for three 50 nm thick $LuFe_2O_4$ films grown on (111) $MgAl_2O_4$, (111) MgO, and (0001) 6H-SiC. Asterisks (*) indicate XRD peaks from the substrates.

Cross-sectional high angle annular dark field scanning transmission electron microscopy (HAADF-STEM) images were recorded on a 100 keV Nion UltraSTEM. The magnetic properties were measured by a Quantum Design superconducting quantum interference device (SQUID) magnetometer in the temperature range from 1.8 to 350 K and magnetic fields up to 70 kOe. RHEED observations provided a convenient indication of proper $LuFe_2O_4$ phase formation during deposition. Undesired FeO_x phases are readily seen by RHEED in the form of spot patterns while the $LuFe_2O_4$ phase appears as streaks, indicating a smooth film surface. Since the film oxygen stoichiometry is difficult to quantify, the films may be oxygen deficient, which could affect properties as in the case with YFe_2O_4.[23]

The layered $LuFe_2O_4$ film structure was confirmed by XRD, displayed in Fig. 2, showing that the $LuFe_2O_4$ films are (0001) oriented and single phase. Despite excess iron being supplied during growth, no iron-rich phases are observed in the films when deposited at 850 °C. Some of this excess iron has been observed by RBS to diffuse into the $MgAl_2O_4$ and MgO substrates. The $LuFe_2O_4$ film lattice

This article is copyrighted as indicated in the article. Reuse of AIP content is subject to the terms at: http://scitation.aip.org/termsconditions. Downloaded to IP: 128.84.143.26 On: Mon, 27 Apr 2015 14:52:39

TABLE I. $LuFe_2O_4$ film lattice parameters and rocking curve full width at half maximum (FWHM) values determined from XRD data.

Substrate	$LuFe_2O_4$ film *c*-axis (Å)	$LuFe_2O_4$ film *a*-axis (Å)	Rocking curve FWHM(°)
(111) MgO	25.42 ± 0.01	3.40 ± 0.02	1.13
(111) $MgAl_2O_4$	25.28 ± 0.01	3.42 ± 0.02	0.76
(0001) 6H-SiC	25.19 ± 0.01	3.44 ± 0.02	0.64

constants and rocking curve results are reported in Table I. The epitaxial orientation relationships between the film and the substrate were verified by ϕ-scans of the $10\bar{1}4$ $LuFe_2O_4$ film peak; the [100] $LuFe_2O_4$ was found to be parallel to $[1\bar{1}0]$ MgO, $[2\bar{1}\bar{1}]$ $MgAl_2O_4$, and [100] 6 H-SiC for the substrates studied.

Figure 3 shows STEM images of the interface between the $LuFe_2O_4$ film and the $MgAl_2O_4$ substrate viewed down the [100] zone axis of the $LuFe_2O_4$ film. Notably, the film is single-phase and free of FeO_x impurity phases at the interface. Figure 3(b) shows a high-resolution image of the film, demonstrating the clear repetition of bright $LuO_{1.5}$ layers (called U layers[24]) with the darker $Fe_2O_{2.5}$ layers (referred to as W layers[24]), each of which contains two atomically resolved Fe-O planes.

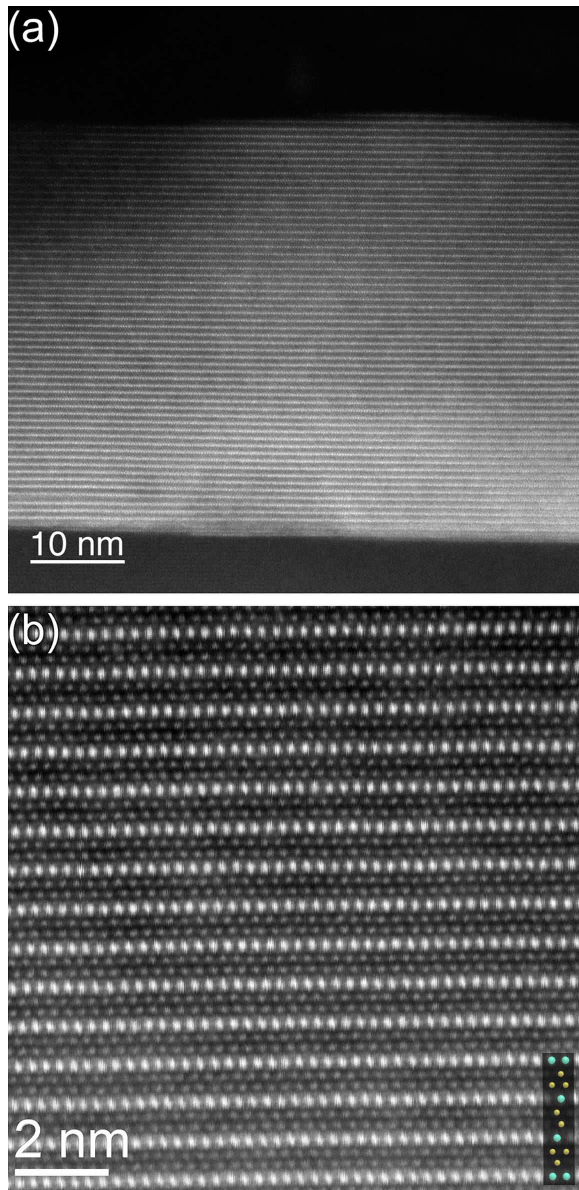

FIG. 3. HAADF-STEM images of the same $LuFe_2O_4$ on $MgAlO_4$ film studied in Fig. 2(d) showing (a) the presence of a clean interface and (b) the well-ordered structure of $LuO_{1.5}$ U layers alternating with $Fe_2O_{2.5}$ W layers. An overlay of a single unit cell is shown in the lower corner of (b).

Magnetization as a function of temperature, displayed in Fig. 4(a), shows that the samples exhibit a singular rapid increase in magnetization below 240 K that is consistent with the bulk paramagnetic to ferrimagnetic phase transition of $LuFe_2O_4$.[25] The samples also display hysteretic behavior with magnetic field, as shown in Fig. 4(b). At 70 kOe, a magnetic moment of about 0.8, 0.3, and 0.1 μ_B per Fe is induced in the films on SiC, $MgAl_2O_4$, and MgO, respectively. The reduced magnetization in the $LuFe_2O_4$ film on $MgAl_2O_4$ and MgO compared to the film on SiC may be due to diffusion of Mg from the substrate into the film since Mg doping has been reported to have this effect.[26] The saturation magnetization in our films is lower than the reported bulk value of $\sim 1.4\ \mu_B$/Fe at 145 kOe.[27] While this difference in magnetic moment may be due to the strong dependence on field cooling observed in bulk $LuFe_2O_4$,[27] other factors relating to the deposition process, such as the creation of oxygen vacancies, might be partially responsible. In addition, the samples do not exhibit superparamagnetism, which has been observed in films containing hexagonal $LuFeO_3$ impurities.[12]

Figure 5 displays the *ab*-plane optical response of $LuFe_2O_4$ in epitaxial thin film form on $MgAl_2O_4$ compared with bulk single crystal data.[28] Comparison with first

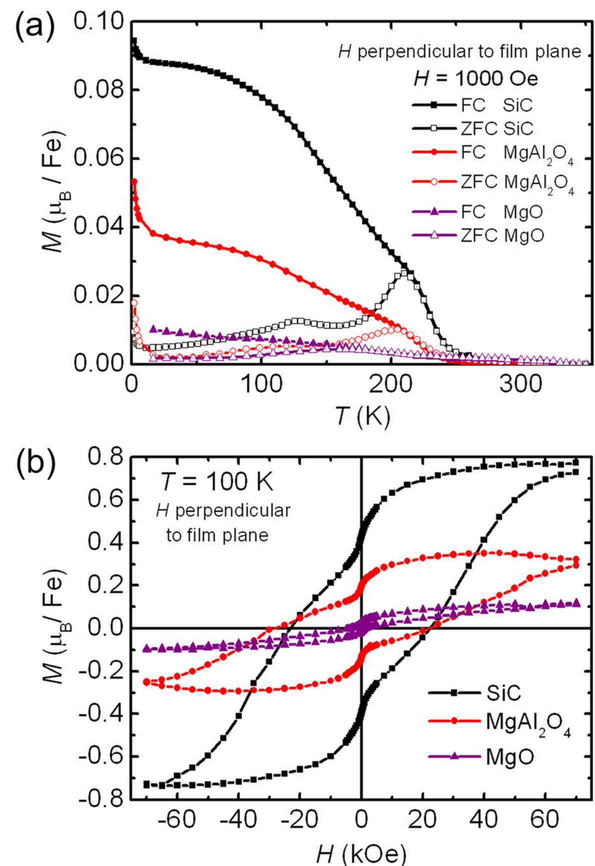

FIG. 4. The magnetization as a function of temperature and magnetic field of the same $LuFe_2O_4$ films as in Fig. 2(d).

This article is copyrighted as indicated in the article. Reuse of AIP content is subject to the terms at: http://scitation.aip.org/termsconditions. Downloaded to IP: 128.84.143.26 On: Mon, 27 Apr 2015 14:52:39

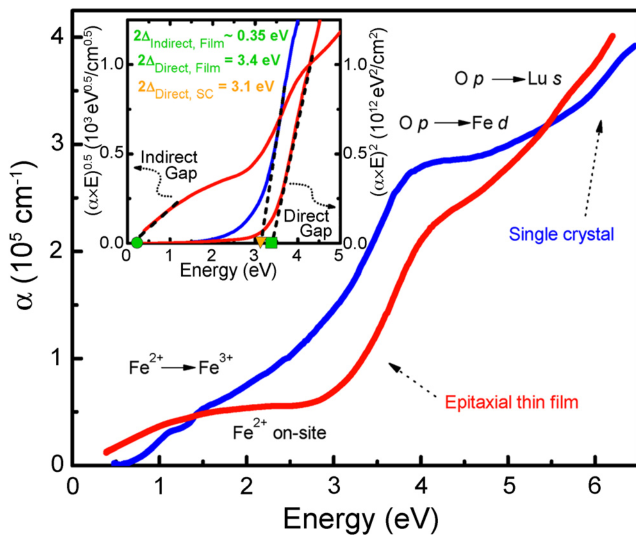

FIG. 5. Optical response of a 75 nm thick (0001) $LuFe_2O_4$ film grown on (111) $MgAl_2O_4$ along with the *ab*-plane response of a $LuFe_2O_4$ single crystal (Ref. 28) at 300 K. The film absorption was determined by a combination of direct calculation of absorption from transmittance (below ~3 eV) and a Glover-Tinkham analysis of both transmittance and reflectance to obtain absorption above 3 eV. The data were merged between 2.5 and 3 eV, where there was substantial overlap. The inset shows the indirect and direct band gap analysis.

principles calculations allows us to assign the observed excitations.[29] The band centered at ~4 eV and the rising higher energy absorption can be assigned as a combination of O *p* → Fe *d* and O *p* → Lu *s* charge transfer excitations. A plot of $(\alpha \times E)^2$ vs. energy places the direct band gap at ~3.4 eV. While the film is not fully commensurate, the average in-plane lattice constant of the film on $MgAl_2O_4$ from XRD is 3.42 ± 0.02 Å, which is 0.6% smaller than the bulk value of 3.44 Å. This compressive strain blue-shifts the direct charge gap and the band maximum compared to similar structures in the single crystal. $BiFeO_3$ displays similar behavior.[30] Previous measurements on single crystalline $LuFe_2O_4$ also identified an indirect band gap at ~0.35 eV, a feature that is defined by the leading edge of the $Fe^{2+} \rightarrow Fe^{3+}$ charge transfer excitations that occur in the W layer (the iron oxide double layer).[28] The film shows a similar, but somewhat leakier tendency in the $(\alpha \times E)^{0.5}$ vs. energy plot, although due to limited optical density, our uncertainties are larger. Similar measurements on a film on SiC are less interpretable due to the 3.05 eV band gap of the substrate.

In summary, we have identified a reliable method for depositing single-phase epitaxial $LuFe_2O_4$ films. This ability combined with the knowledge that the charge-order transition temperature of $LuFe_2O_4$ is sensitive to pressure[31] invites the use of thin film methods, e.g., strain or dimensional confinement through heterostructuring, to modify the structure and properties of this controversial multiferroic.

Research supported by the U.S. Department of Energy, Office of Basic Energy Sciences, Division of Materials Sciences, and Engineering under Award Nos. DE-SC0002334 (sample synthesis and characterization) and DE-FG02-01ER45885 (spectroscopy). C.M.B. acknowledges stipend support from the National Science Foundation through the MRSEC program (DMR-0820404). J.A.M. acknowledges financial support from a National Defense Science & Engineering Graduate Fellowship. Electron microscopy facility support through the NSF MRSEC program (DMR 1120296) and NSF IMR-0417392. We thank P. Chen for useful discussions.

[1] N. A. Hill, J. Phys. Chem. B **104**, 6694–6709 (2000).
[2] S.-W. Cheong and M. Mostovoy, Nature Mater. **6**, 13–20 (2007).
[3] N. Ikeda, H. Ohsumi, K. Ohwada, K. Ishii, T. Inami, K. Kakurai, Y. Murakami, K. Yoshii, S. Mori, Y. Horibe, and H. Kito, Nature **436**, 1136–1138 (2005).
[4] J. de Groot, T. Mueller, R. A. Rosenberg, D. J. Keavney, Z. Islam, J.-W. Kim, and M. Angst, Phys. Rev. Lett. **108**, 187601 (2012).
[5] A. Ruff, S. Krohns, F. Schrettle, V. Tsurkan, P. Lunkenheimer, and A. Loidl, Eur. Phys. J. B **85**, 290 (2012).
[6] J. de Groot, K. Marty, M. D. Lumsden, A. D. Christianson, S. E. Nagler, S. Adiga, W. J. H. Borghols, K. Schmalzl, Z. Yamani, S. R. Bland, R. de Souza, U. Staub, W. Schweika, Y. Su, and M. Angst, Phys. Rev. Lett. **108**, 037206 (2012).
[7] X. S. Xu, J. de Groot, Q.-C. Sun, B. C. Sales, D. Mandrus, M. Angst, A. P. Litvinchuk, and J. L. Musfeldt, Phys. Rev. B **82**, 014304 (2010).
[8] J. H. Haeni, P. Irvin, W. Chang, R. Uecker, P. Reiche, Y. L. Li, S. Choudhury, W. Tian, M. E. Hawley, B. Craigo, A. K. Tagantsev, X. Q. Pan, S. K. Streiffer, L. Q. Chen, S. W. Kirchoefer, J. Levy, and D. G. Schlom, Nature **430**, 758–761 (2004).
[9] K. J. Choi, M. Biegalski, Y. L. Li, A. Sharan, J. Schubert, R. Uecker, P. Reiche, Y. B. Chen, X. Q. Pan, V. Gopalan, L.-Q. Chen, D. G. Schlom, and C. B. Eom, Science **306**, 1005–1009 (2004).
[10] R. Rejman, T. Dhakal, P. Mukherjee, S. Hariharan, and S. Witanachchi, in *Multiferroic and Ferroelectric Materials*, edited by A. Gruverman, C. J. Fennie, I. Kunishima, B. Noheda, and T. W. Noh, (Mater. Res. Soc. Symp. Proc., 2010), Vol. 1199, p. F03–22.
[11] J. Liu, Y. Wang, and J. Y. Dai, Thin Solid Films **518**, 6909–6914 (2010).
[12] W. Wang, Z. Gai, M. Chi, J. D. Fowlkes, J. Yi, L. Zhu, X. Cheng, D. J. Keavney, P. C. Snijders, T. Z. Ward, J. Shen, and X. Xu, Phys. Rev. B **85**, 155411 (2012).
[13] J. R. Arthur, J. Appl. Phys. **39**, 4032 (1968).
[14] A. Y. Cho, J. Appl. Phys. **41**, 2780 (1970).
[15] A. Y. Cho, J. Appl. Phys. **42**, 2074 (1971).
[16] C. Theis and D. G. Schlom, Thin Solid Films **325**, 107–114 (1998).
[17] J. F. Ihlefeld, A. Kumar, V. Gopalan, D. G. Schlom, Y. B. Chen, X. Q. Pan, T. Heeg, J. Schubert, X. Ke, P. Schiffer, J. Orenstein, L. W. Martin, Y. H. Chu, and R. Ramesh, Appl. Phys. Lett. **91**, 071922 (2007).
[18] M. Seki, T. Konya, K. Inaba, and H. Tabata, Appl. Phys. Express **3**, 105801 (2010).
[19] Z. K. Liu, J. Phase Equilib. Diffus. **30**, 517–534 (2009).
[20] J. O. Andersson, T. Helander, L. Hoglund, P. Shi, and B. Sundman, CALPHAD: Comput. Coupling Phase Diagrams Thermochem. **26**, 273–312 (2002).
[21] These mismatch values correspond to the observed epitaxial orientation relationship for these systems (described in Fig. 2), where we have assumed near-coincident site lattices (NCSL) with σ-boundary ratios at the interfaces of $\sigma_{MgO}1 : \sigma_{LuFe_2O_4}1$, $\sigma_{MgAl_2O_4}1 : \sigma_{LuFe_2O_4}3$, and $\sigma_{SiC}1 : \sigma_{LuFe_2O_4}1$. The areas of the NCSL unit cells for these cases are 0.077 nm^2, 0.283 nm^2, and 0.081 nm^2, respectively. For additional information on NCSL, see Ref. 22.
[22] R. W. Balluffi, A. Brokman, and A. H. King, Acta Metall. **30**, 1453–1470 (1982).
[23] M. Inazumi, Y. Nakagawa, M. Tanaka, N. Kimizuka, and K. Siratori, J. Phys. Soc. Jpn. **50**, 438–444 (1981).
[24] T. Sugihara, K. Siratori, N. Kimizuka, J. Iida, H. Hiroyoshi, and Y. Nakagawa, J. Phys. Soc. Jpn. **54**, 1139–1145 (1985).
[25] J. Wen, G. Xu, G. Gu, and S. M. Shapiro, Phys. Rev. B **80**, 020403(R) (2009).
[26] Y. B. Qin, H. X. Yang, Y. Zhang, H. F. Tian, C. Ma, Y. G. Zhao, R. I. Walton, and J. Q. Li, J. Phys.: Condens. Matter **21**, 015401 (2009).
[27] J. Iida, M. Tanaka, Y. Nakagawa, S. Funahashi, N. Kimizuka, and S. Takekawa, J. Phys. Soc. Jpn. **62**, 1723–1735 (1993).
[28] X. S. Xu, M. Angst, T. V. Brinzari, R. P. Herman, J. L. Musfeldt, A. D. Christianson, D. Mandrus, B. C. Sales, S. McGill, J.-W. Kim, and Z. Islam, Phys. Rev. Lett. **101**, 227602 (2008).
[29] H. J. Xiang and M.-H. Whangbo, Phys. Rev. Lett. **98**, 246403 (2007).
[30] P. Chen, N. J. Podraza, X. S. Xu, A. Melville, E. Vlahos, V. Gopalan, R. Ramesh, D. G. Schlom, and J. L. Musfeldt, Appl. Phys. Lett. **96**, 131907 (2010).
[31] X. Shen, C. H. Xu, C. H. Li, Y. Zhang, Q. Zhao, H. X. Yang, Y. Sun, J. Q. Li, C. Q. Jin, and R. C. Yu, Appl. Phys. Lett. **96**, 102909 (2010).

This article is copyrighted as indicated in the article. Reuse of AIP content is subject to the terms at: http://scitation.aip.org/termsconditions. Downloaded to IP: 128.84.143.26 On: Mon, 27 Apr 2015 14:52:39